Journal of Electroceramics, 13, 829–837, 2004

Effect of B_2O_3 Nano-Coating on the Sintering Behaviors and Electrical Microwave Properties of $Ba(Nd_{2-x}Sm_x)Ti_4O_{12}$ Ceramics

LI-CHUN CHANG[1,*] & BI-SHIOU CHIOU[2]

[1] *Department of Electronics Engineering and Institute of Electronics, National Chiao Tung University, 1001 Ta Hsueh Rd., Hsinchu, 300, Taiwan, Republic of China*

[2] *Department of Electronics Engineering and Institute of Electronics, National Chiao Tung University, 1001 Ta Hsueh Rd., Hsinchu, 300, Taiwan, Republic of China*

Submitted February 12, 2003; Revised April 16, 2004; Accepted April 26, 2004

Abstract. $Ba(Nd_{0.8}Sm_{0.2})_2Ti_4O_{12}$ ceramics prepared by conventional solid-state sintering have a dielectric constant of about 80 and a nearly zero temperature coefficient of resonant frequency; however, the sintering temperature is above 1350°C. Doping with B_2O_3 (up to 5 wt%) promotes the densification and dielectric properties of BNST ceramics. It is found that coating BNST powder with thin B_2O_3 layer of about 180 nm reduces the sintering temperature to below 1020°C. The effects of B_2O_3 nano-coating on the dielectric microwave properties and the microstructures of BNST ceramics are investigated. Ninety-six percent of theoretical densities is obtained for specimens coated with 2 wt% B_2O_3 sintered at 960°C and the samples exhibit significant (002) preferred orientation and columnar structure.

Keywords: oxide, microwave dielectric properties, ceramics, liquid phase sintering

1. Introduction

As the rapid development in telecommunications and microelectronic technology, dielectric materials are continuing to play a very important role. These materials are key in realization of low-loss temperature-stable resonators and filters for broadcasting equipments, and in many other microwave devices. High dielectric-constant materials are critical to miniaturization of wireless system, both for the terminals and base-stations, as well as for handsets [1, 2]. The BaO-PbO-Nd_2O_3-TiO_2 material has a dielectric constant as high as 88 at 1 GHz [3]. It is widely used at frequencies of around 1 GHz. Its Q value of 5000 is high enough for use at frequencies smaller than 1 GHz, but with lead-pollution concern. Processes of BaO-Nd_2O_3-TiO_2 series materials were, however, extremely difficult due to complicated interactions between the constituents [4]. The dielectric properties were not sensitive with minor deviations of Nd_2O_3 content; however, the temperature stability and phase composition were sensitive to the ratio of TiO_2/BaO. Kolar et al. [4] used Bi_2O_3 to improve the temperature coefficient of resonant frequency of $BaO{\cdot}Nd_2O_3{\cdot}5TiO_2$. A sintering temperature of 1350–1370°C is needed to obtain a ceramic disc with good dielectric properties of $k = 105$ and $Q = 1000$ at 1 MHz, however, the temperature coefficient of resonant frequency (τ_f) is very high (−104 ppm/°C). Laffez [5] sintered BaO-(Nd_2O_3, Sm_2O_3)-TiO_2 system at 1400°C and obtained a k of 74 to 81, a $Q \times f$ of up to 9000 GHz at 3 GHz, and a τ_f of around +9 ppm/°C. They found that addition of 1 or 2 wt% WO_3, MnO_2, and CaO to two compositions of the BaO-(Nd_2O_3, Sm_2O_3)-TiO_2 system densified ceramics and improved the microwave properties. The WO_3 and MnO doped ceramics show a large dielectric constant, accompanied second phase and lower $Q \times f$ value, however, the sintering temperatures are above 1350°C.

Chemical processing and small particle sizes of the starting materials are generally advantageous to reduce the sintering temperature of dielectric materials

*To whom all correspondence should be addressed. E-mail: lcchang.ee87g@nctu.edu.tw

[6, 7]. However, they required a complex procedure that increased the cost and time to fabricate a dielectric device. Attrition milling produces very fine powders that allow for good densification but with the risk of contamination. The liquid phase sintering by adding glass or other low melting point materials was found to effectively lower the firing temperature of ceramics [6]. The dielectric microwave properties of dielectric resonators were deeply affected by the liquid phase, the sintering temperature and the reactions between host material and additives. In this study, B_2O_3 was chosen as a sintering aid to lower the sintering temperature of $Ba(Nd_{0.8}Sm_{0.2})_2Ti_4O_{12}$ (hereafter referred to as BNST) ceramics. The crystalline phase, the microstructures, and the dielectric microwave properties of B_2O_3-added BNST ceramics are investigated.

2. Experiments

Host material (BNST) powders were mixed with x wt% ($x = 0$–5) reagent grade B_2O_3(>99% purity) powders and distilled water. The mixture was stirred at 90°C for 3 hr. After cooling, the mixture was milled for 12 hr with zirconia balls. Then the slurry was dehydrated and granulated by mixing with 3 wt% polyvinyl alcohol solution. Pellets with 10mm in diameter and either 5.2 or 1.2 mm in thickness were pressed using a uni-axis press at 750 kg/cm^2. Then the pellets were sintered in the temperature range of 900–1100°C for 1.0 hr in air.

The X-ray diffraction spectra were collected by using Cu K_α ($\lambda = 0.15406$ nm) radiation with 30 kV and 20 mA in the 2θ range of 20 to 50° (XRD, MAC science MXP18), the intensity of the main peak was then integrated. The microstructure observations of sintered samples were performed by scanning electron microscope (SEM, Hitachi S4700) and transmission electron microscope (TEM, Hitachi H-7500). The SEM observations were performed on the as-sintered surfaces. An electron probe microanalyzer (EPMA, Joel JXA-8800M) was used to analyze the composition of the sintered samples. The bulk densities of the sintered specimens were measured by the Archimedes' method. According to the rule of mixing, the density of BNST-B_2O_3 ceramics is calculated as following:

$$D_{\text{cal}} = (W_1 + W_2)/(W_1/D_1 + W_2/D_2) \qquad (1)$$

where W_1 and W_2 are the weights of the BNST dielectric and B_2O_3 in the mixtures, respectively; D_1 and D_2 are the theoretical densities of the BNST and B_2O_3, respectively. The dielectric characteristics were measured with an Impedance/Gain-Phase Analyzer (HP4194, Hewlett Packard Co.) in the frequency range of 100 Hz–15 MHz. Silver paste was used for the electrodes. The dielectric constant (k) and the quality factor ($Q \times f$) at microwave frequencies were measured using the Hakki-Coleman dielectric resonator method which was modified and improved by Courtney [8]. The dielectric resonator was positioned between two brass plates. A system combined with a HP8510 network analyzer and a HP8350 sweep oscillator was employed in the measurement. The $Q \times f$ factor was used for evaluating the loss quality, where f is the resonant frequency.

3. Results and Discussion

X-ray diffraction patterns for BNST specimens with various contents of B_2O_3 and sintered at 960–1100°C for 1.0 hr are shown in Fig. 1. No interaction between B_2O_3 and BNST is observed. The only phase detected is $Ba(Nd_{0.8}Sm_{0.2})_2Ti_4O_{12}$ for the entire sintering temperature range. However, the intensity of (002) peak increases with the increase of B_2O_3 content and/or the raise of sintering temperature, as exhibited in Fig. 1. For 5 wt% B_2O_3 added sample, the main peak is (002). With increasing sintering temperature, the intensities of the all structure characteristic peaks increase and the preferred orientation becomes (002) for the B_2O_3 added BNST samples. The transition of preferred orientation was not observed on the un-doped BNST ceramics, sintered at temperature range of 1150–1450°C, as exhibited in Fig. 2.

The crystallographic texture of B_2O_3-doped BNST is affected by both the sintering temperature and the B_2O_3 content. The peak intensity ratio (R) of $I_{(002)\text{-sintered}}/I_{(002)\text{-unsinteredpellet}}$ increases with the increase of boric oxide contents and/or the sintering temperature. As shown in Fig. 3(a), an R of 17.6 is obtained for 5 wt% B_2O_3 specimen sintered at 1100°C as compared to that of 1.4 for 1 wt% B_2O_3 specimen sintered at 900°C. However, no apparent difference in R is observed among the undoped samples sintered in the temperature of 1300–1650 K. Figure 3(b) exhibits a linear relationship between $\ln(R)$ and $1/T$, and this suggests a diffusion-controlled growth-mechanism [9]. It is found that the intensity ratio $R(R \equiv I_{002}(x, T)/I_{002}(0, 298))$ is a function of both the B_2O_3 content x and the sintering temperature $T(K)$, and can be fitted with the

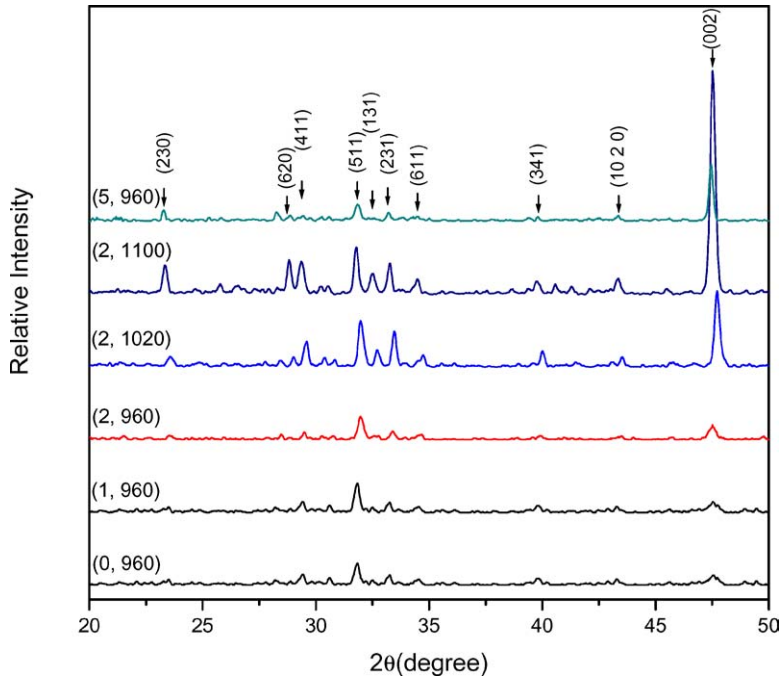

Fig. 1. XRD patterns for BNST ceramics doped with x wt% B_2O_3 and sintered at temperature T°C for 1.0 hr. Data in the parenthesis are x and T, i.e., (x, T).

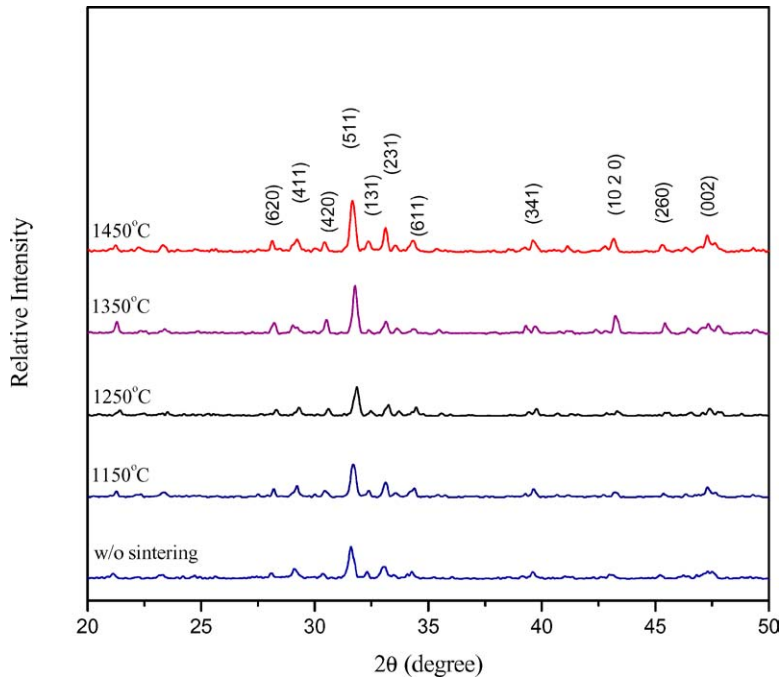

Fig. 2. XRD patterns for un-doped BNST ceramics sintered at various temperatures in air for 2.0 hr.

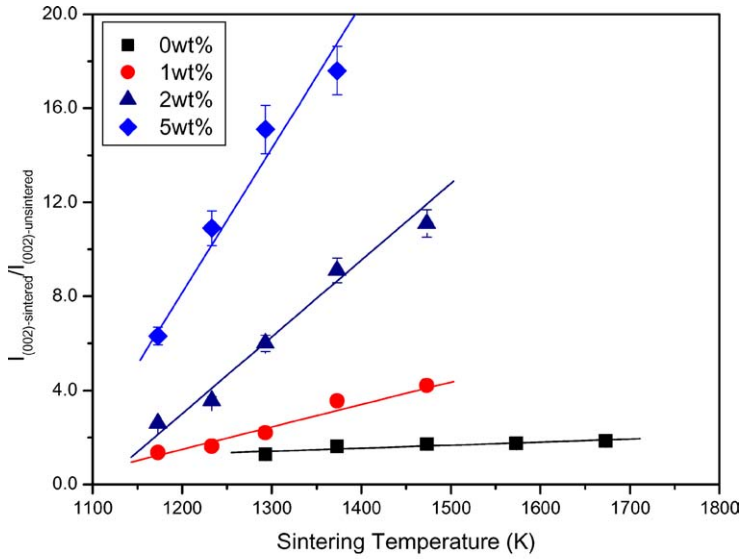

(a)

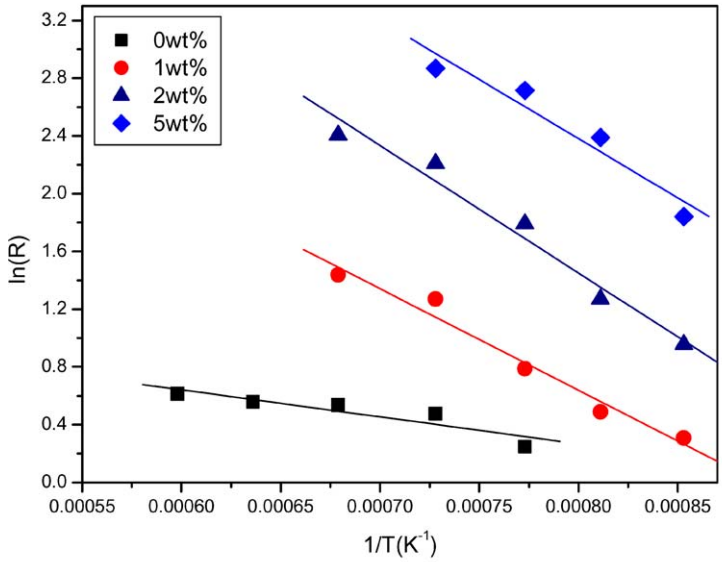

(b)

Fig. 3. (a) Intensity ratios (R) of $I_{(002)\text{-sintered}}/I_{(002)\text{-unsintered}}$ as a function of sintering temperature for the specimens with x wt% B_2O_3 contents sintered for 1.0 hr in air. (b) The plots are $\ln(R)$ vs. the reciprocal of temperature $(1/T)$.

Arrhenius equation as following:

$$R = f(x, T) \sim A(x) \exp(-E_a/kT) \qquad (2)$$

where $A(x)$ is a pre-exponential factor, E_a is the activation energy, and k is the Boltzmann constant. Table 1 summarized the A and E_a obtained from the plots of Fig. 3(b). The pre-exponential factor $A(x)$ is proportional to x and $A(x) \approx 1535x + 5$. The activation energies are ~70 kJ/mole for the boric oxide doped BNST and 16 kJ/mole for undoped one. A smaller activation energy of the undoped specimen suggests a

Table 1. The pre-exponential (A) and activation energy (E_a) obtained from the plots of Fig. 3(b).

x wt% (B_2O_3 content)	$A(x)$	E_a (kJ/mole)
0	5.83	16 ± 3.2
1	1438.06	68 ± 6.1
2	3142.27	70 ± 6.4
5	7648.00	69 ± 6.2

$A(x) \sim 1535x + 5$

short circuit diffusion path, such as: surface diffusion. Doping of B_2O_3 raises the activation energy, however, a constant activation energy (∼70 kJ/mole) is obtained for samples doped with various amount of B_2O_3. The melting point of B_2O_3 is ∼480°C. It is argued that the presence of the liquid sintering aid (i.e., B_2O_3) along the grain boundaries alters the dominant diffusion path from the short diffusion path to a longer diffusion path, such as, grain boundary diffusion. Hence, a larger activation is obtained for the B_2O_3-doped specimens. Further doping did not change the E_a because the dominant diffusion path is the same for all the B_2O_3-doped samples. The increase of R with x is attributed to the linear relationship between the pre-exponential term $A(x)$ and the boron content x. During liquid phase sintering, a wetting liquid creates an attractive force between particles, putting the particles contact in compression. Further, packing irregularities produce shear at the particle contact that aids rearrangement. The particles instantaneously repack to higher coordination, with melt spreading between the particles [10]. The rearrangement process is more efficient when more liquid is present. Hence, $\ln(R)$ increases with the increase of B_2O_3.

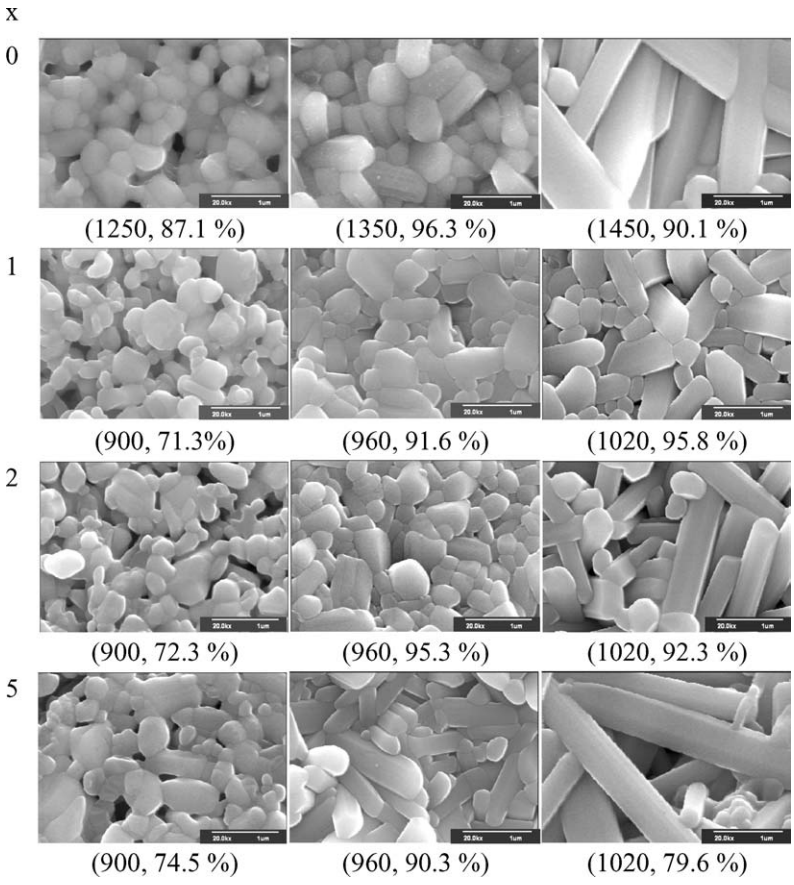

Fig. 4. SEM micrographs of BNST ceramics with x wt% B_2O_3 contents sintered in air for 1.0 hr at temperature T°C, and the relative density ($D_r = D_{\text{measured}}/D_{\text{calculated}} \times 100\%$). Data in parenthesis are T and D_r, i.e., (T, D_r).

The SEM micrographs of BNST ceramics with various amounts of B_2O_3 and sintered at different temperatures are shown in Fig. 4. The undoped BNST ceramics achieves 96% theoretical density (D_{th}) when sintered at 1350°C for 1.0 hr. While those sintered at higher temperature (1450°C) exhibits columnar structure and lower density (90% D_{th}). Those at lower temperature (1250°C) are granular and porous (87% D_{th}). The 1450°C-sintered samples exhibit a columnar feature accompanying voids and the abnormal grain is over 5 μm in length and 0.35 μm in diameter. Chen et al. [11] argued that the BNST system acquired little liquid phase when sintering temperature reached or exceeded 1350°C because BNST ceramics had a eutectic temperature between 1350 and 1375°C. The liquid phase would improve the density and the columnar grain growth of the sintered specimens. They also report a decrease of density when the sintering temperature exceeds 1360°C. The measured densities of 1 wt% B_2O_3-BNST sintered at temperatures ranged from 900 to 1100°C for 1.0 hr were 71.3–95.8% of the calculated densities. Nearly equi-axis fine crystals, i.e., crystals with more rounded grains, were observed in the undoped-BNST ceramics sintered below 1150°C, while specimens with 1 wt% B_2O_3 sintered at 1100°C for 1.0 hr in air reveal columnar structure. At higher concentrations of boron (>1 wt%) the directional grain growth becomes distinctly visible. The tendency to directional grain growth becomes stronger at higher boron concentrations. Samples with more than 2 wt% B_2O_3 sintered at 1020°C are composed of exclusively elongated grains. While for the undoped samples, granular grain boundaries were the predominant ones except for those sintered at 1450°C and above. The formation of columnar structure is apparent for specimens doped with 5 wt% (i.e., 9.23 vol%) B_2O_3 at a sintering temperature of as low as 960°C. Exaggeratedly grown columnar structure with a preferred orientation of (002) is observed, especially for samples with 5 wt% B_2O_3 sintered at 1020°C. This implies that B_2O_3 both reduces the sintering temperature of the dielectric ceramics and contributes to (002) preferred orientation due to the liquid phase during the sintering process.

The ratios of length to diameter of the columnar grain, l/d, increase with the sintering temperature in the range of 900 to 1100°C for B_2O_3-added specimens, as shown in Fig. 5. The value of l/d also increases as the amount of B_2O_3 increases. In the classic liquid-phase sintering, rearrangement, solution-reprecipitation, and final-stage sintering are the three stages of densification [10]. It seems that the additive content up to 2 wt%

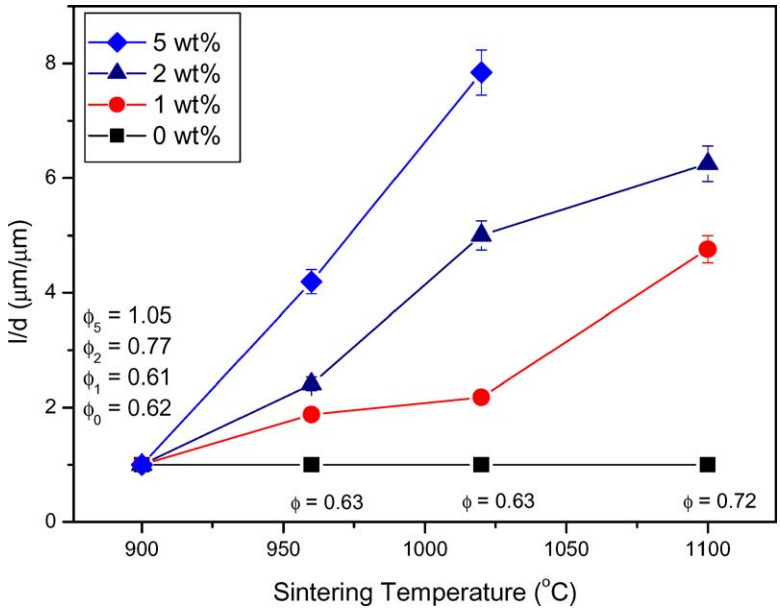

Fig. 5. The ratios of l/d as a function of sintering temperature for the specimens with various B_2O_3 contents sintered for 1.0 hr in air (l and d are the length and diameter of the columnar grain; ϕ is the diameter of the granular grain, unit in μm).

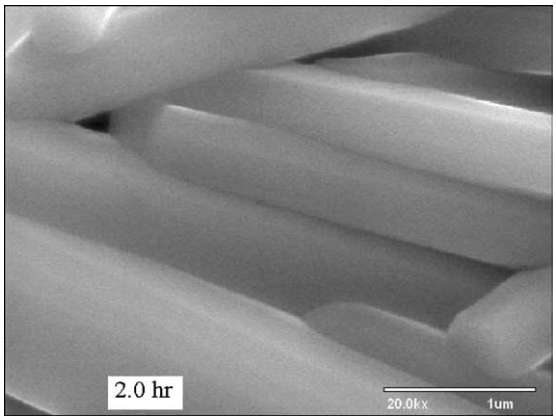

Fig. 6. The grain morphology of BNST ceramics with 5 wt% B_2O_3 sintered at 960°C for 2.0 hr in air.

and sintering temperature above or equal to 960°C were the criterion in this study on liquid formation which implied a burst of rearrangement densification, followed by solution-reprecipitation with concomitant grain growth and grain shape accommodation. The typical columnar structure could be observed for the samples even doped with 1 wt% boric oxide only and sintered at 960°C. And the phenomenon is more evident for the 5 wt% additive ones illustrated in Fig. 6. The sufficient liquid phase brings columnar grains to grow in length and rearrange in preferred orientation - (002) direction. On the contrary, the undoped ceramics sintered under 1100°C revealed porous structure characterized by neck growth of spherical grains.

There are several locations where boron ions could migrate during sintering: incorporated into the grains, segregated at the grain boundaries, resided in a second phase, and/or joined the ambient by evaporation/sublimation. The lattice parameters obtained from the XRD patterns and the calculated volume of unit cell are illustrated in Fig. 7. There is a slight increase of the univolume (<2%) when the sintering temperature raises from 960 to 1100°C. For specimens sintered at 960°C, the univolume increases with the increase of B_2O_3 content, however, no apparent difference of univolume is observed among samples with various B_2O_3 contents when the sintering temperature exceeds 1020°C. The atomic radii of B, Ba, Nd, Sm, Ti and O are 0.023,

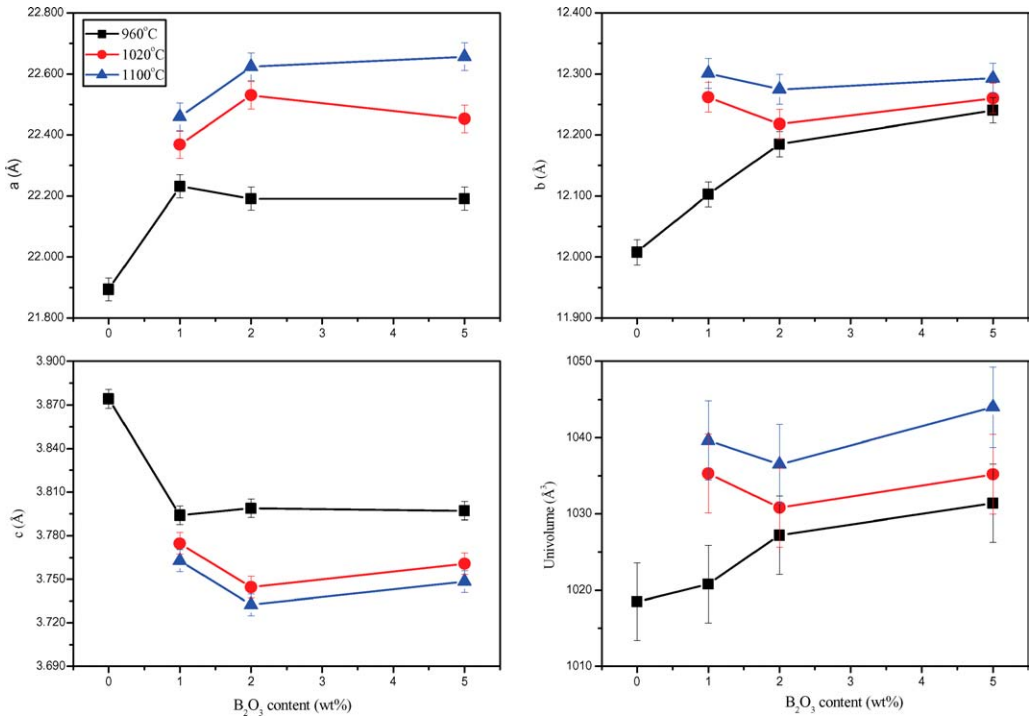

Fig. 7. The lattice parameter a, b, c, and the unit cell volume of BNST ceramics as a function of boric oxide contents, the samples sintered at 960, 1020 and 1100°C for 1.0 hr in air.

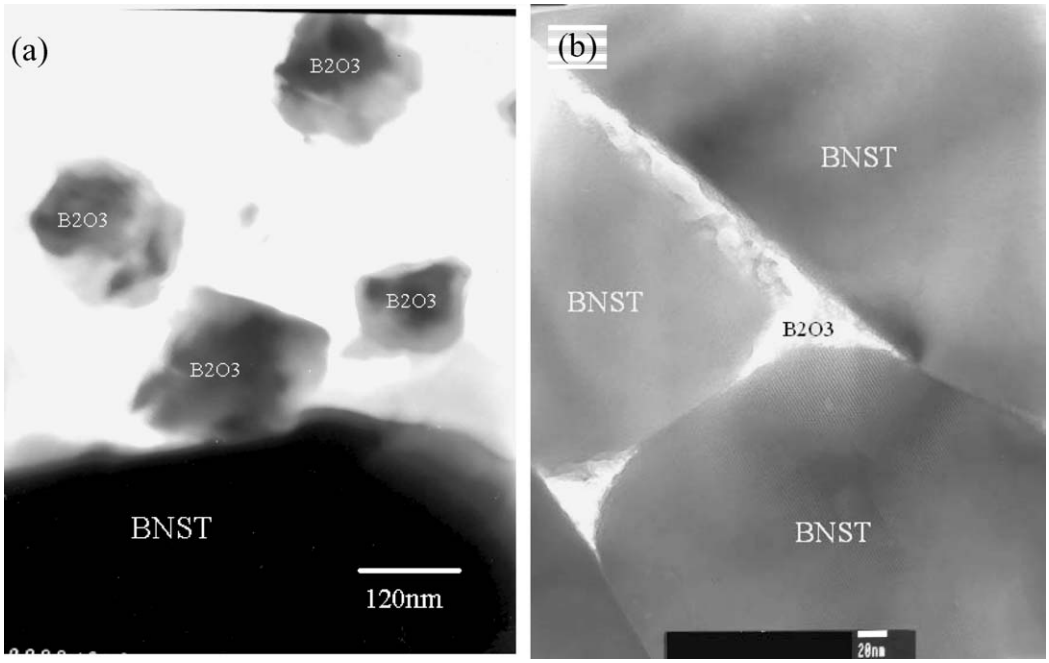

Fig. 8. TEM micrographs of the microstructure of (a) BNST particle surface with 2 wt% B_2O_3 coating, and (b) sintered for 1.0 hr at 960°C in air in the final stage of liquid-phase sintering micrographs.

0.136, 0.100, 0.096, 0.061, and 0.14 nm, respectively. If the small boron atoms would incorporate into the lattice sites, a decrease, instead of increase, of the univolume will be observed. Hence, the increase of the univolume for specimens sintered at higher temperature and/or doped with more B_2O_3 is attributed to the diffusion of B atoms to the interstitial sites.

In sintered specimens, no specific boron compound was observed at grain boundaries, and the EPMA analysis results indicate that the boron content of the 1100°C-sintered specimens is same as that of the unsintered-sample. Maljuk et al. [14] reported that the amount of boron volatilization from the liquid during 12 hr, 1240°C sintering in air is negligible. They annealed pure B_2O_3 in an Al_2O_3 crucible at 1240°C for 12.0 hr in air, the result showed that the volatility of boron was nearly 1.2 wt% per day. In our work, when the sintering temperature is above 1200°C, the bottom of the crucible become grayish black and the presence of boron was confirmed by EPMA analysis. Hence, the B_2O_3-doped BNST should be sintered under 1200°C to have a better control of the boric oxide content of the composition. The TEM micrograph of unsintered B_2O_3-doped BNST powders, shown in Fig. 8(a), suggests that the BNST powders were surrounded by the fine B_2O_3 particles which could form homogeneous liquid phase between the ceramic grains during sintering and provide grain boundary diffusion paths as discussed previously. The columnar grain-fringe image of the sintered pellet, shown in Fig. 8(b), reveals the existence of boric oxide at the grain boundaries.

The dielectric constant (k) and $Q \times f$ value of samples increase initially and then decrease with increasing sintering temperature, as shown in Fig. 9. With 2 wt% B_2O_3 addition, a k value of 50 is obtained for BNST bulk sintered at 960°C. Specimen with 1 wt% B_2O_3 exhibits the highest $Q \times f$ value (∼5500 GHz) and a moderate k (∼43), among all compositions studied. The boric oxide is effective in the densification of BNST ceramics, it reduces the sintering temperature when added appropriately, and enhances the growth of columnar structure with high ratio of length to diameter. However, the role of the columnar microstructure plays in the dielectric microwave properties is very complicated and subjected to further investigation.

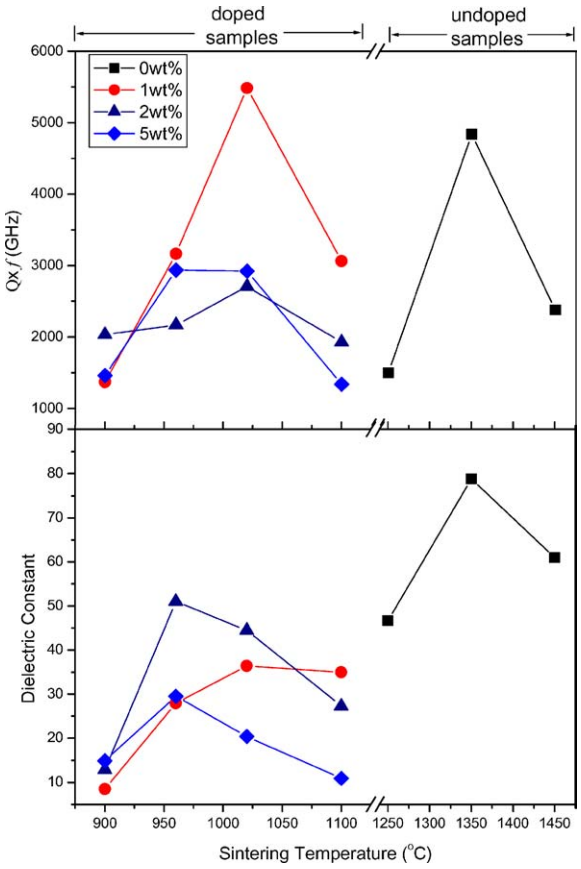

Fig. 9. Dielectric properties as a function of sintering temperature for BNST ceramics with various amounts of B_2O_3 additive sintered in air for 1.0 hr. The sintering time for the un-doped BNST ceramics sintered is 2.0 hr.

Conclusions

In this study, the effects of B_2O_3 on the properties of BNST dielectric are investigated. Ninety-six percent of theoretical densities is obtained for specimens coated with 2 wt% B_2O_3 sintered at 960°C. Addition of boric oxide also influences the microstructure evolution of the dielectric. For samples without B_2O_3, a columnar structure is obtained when the sintering temperature exceeds 1350°C. However, exaggerated columnar grains grow at 1100°C for specimens doped with 1 wt% B_2O_3. For samples with 5 wt% boric oxide, a columnar structure with grain length 8 times longer than grain diameter is obtained. X-ray diffraction patterns show significant (002) preferred orientation. For BNST dielectrics with 1 wt% boric oxide sintered at 1020°C, $Q \times f$ is more than 5500 GHz at 6 GHz, which is equal to that of BNST sintered at 1350°C ($Q \times f = 6000$ GHz at 8 GHz), but the dielectric constant is 43 as compared to 80 of BNST.

Acknowledgments

This work is sponsored by National Science Council, Taiwan, under the contract numbers NSC92-2216-E009-007.

References

1. L.J. Golonka, K.J. Wolter, A. Dziedzic, J. Kita, and L. Rebenklau, *24th International Spring Seminar on Electronics Technology* (IEEE, Romania, 2001), p. 73.
2. S. Jerry Fiedziuszko, Ian C. Hunter, T. Itoh, Y. Kobayashi, T. Nishikawa, S.N. Stitzer, and K. Wakino, *IEEE Trans. Microwave Theory Tech.*, **50**, 706 (2002).
3. K. Wakino, K. Minai, and H. Tamura, *J. Am. Ceram. Soc.*, **67**, 278 (1984).
4. D. Kolar, S. Gaberscek, Z. Stadler, and D. Suvorov, *Ferroelectrics*, **27**, 269 (1980).
5. P. Laffez, G. Desgardin, and B. Raveau, *J. Mater. Sci.*, **27**, 5229 (1992).
6. T. Takada, S.F. Wang, S. Yoshikawa, S.J. Jang, and R. E. Newnham, *J. Am. Ceram. Soc.*, **77**, 1909 (1994).
7. V. Tolmer and G. Desquardin, *J. Am. Ceram. Soc.*, **80**, 1981 (1997).
8. B.W. Hakki and P.D. Coleman, *IRE Transactions on Microwave Theory and Techniques*, **8**, 402 (1960).
9. B.N. Roy, *Crystal Growth from Melts* (John Wiley & Sons, Inc., 1992), p. 304.
10. Randall M. German, *Sintering Theory and Practice* (John Wiley & Sons, Inc., 1996), p. 225.
11. X.M. Chen, Y. Suzuki, and N. Sato, *J. Mat. Sci.: Materials in Electrics*, **6**, 10 (1995).
12. L.C. Chang, B.S. Chiou, and W.H. Lee, *J. Mat. Sci.: Materials in Electrics*, **15**, 153 (2004).
13. R.D. Shannon and C.T. Prewitt, *Acta Cryst.*, **B25**, 925 (1969).
14. A. Maljuk, S. Watauchi, I. Tanaha, and H.K. Kojima, *Journal of Crystal Growth*, **212**, 138 (2000).